11-1982

Subharmonic Generation by Resonant Three-Wave Interaction of Deep-Water Capillary Waves

Partha P. Banerjee
University of Dayton, pbanerjee1@udayton.edu

Adrianus Korpel
University of Iowa

Subharmonic generation by resonant three-wave interaction of deep-water capillary waves

P. P. Banerjee and A. Korpel
Department of Electrical and Computer Engineering, The University of Iowa, Iowa City, Iowa 52242

(Received 28 May 1982; accepted 14 July 1982)

Subharmonic generation has been observed during the propagation of deep-water capillary waves. The observations are shown to be in agreement with the theory of degenerate resonant noncollinear three-wave interaction in a nonlinear, dispersive medium.

I. INTRODUCTION

The mechanism for nonlinear resonant interaction between two or more wavetrains traveling on the surface of deep water has been extensively studied over the last two decades, particularly by Phillips,[1] Longuet-Higgins,[2] and McGoldrick.[3] It can be shown[4] that, in general, three-wave interactions, either collinear or noncollinear, cannot occur for deep-water gravity waves, because it is impossible to find closed triads of wavenumbers satisfying the resonance conditions, viz., the simultaneous solutions of the equations $\bar{k}_1 \pm \bar{k}_2 = \bar{k}_3$ and $\omega_1 \pm \omega_2 = \omega_3$, where ω_i is the (angular) frequency corresponding to the wavevector $\bar{k}_i$ and $|\bar{k}_i| < k^* = (g\rho/2T)^{1/2}$ where T is the surface tension, ρ the density of the water, and g is the acceleration due to gravity. However, in the range $|\bar{k}_i| > k^*$, which is our concern in this paper, the dispersion relation $\omega = (gk_i + Tk_i^3)^{1/2}$ allows noncollinear interaction.

Second harmonic generation due to resonant collinear interaction of capillary-gravity waves in water has been observed by McGoldrick.[4] Also, evolution equations have been developed for the interacting amplitudes for the general noncollinear interaction case[3] and solved for the degenerate case of second harmonic generation. These exact solutions indicate a resonant transfer of energy from the fundamental to the second harmonic resulting in gradual decay of the fundamental and an asymptotic increase in the amplitude of the second harmonic with time. The equations are, however, modified by the presence of viscous, dissipative effects in the medium and only approximate solutions can then be obtained.

In this paper, we report on a simple experiment using deep-water capillary waves for which subharmonic generation is observed due to noncollinear resonant three-wave interaction. The subharmonic wavefronts at a particular frequency propagate away from the fundamental at an angle that can be predicted from the resonant triad wavevector diagram. Explicit expressions for the evolution of the fundamental and subharmonic amplitudes have been derived starting from McGoldrick's generalized equations for the three interacting wave amplitudes.[3] The expressions predict growth of the subharmonic followed by a subsequent decay and consequent regeneration of the fundamental. Experimental observations are in good agreement with the theoretical predictions.

II. EXPERIMENTAL SETUP AND INITIAL OBSERVATIONS

In order to generate and monitor capillary waves on the surface of water we employ the experimental setup as shown in Fig. 1. The waves are generated on the surface of ordinary untreated tap water, contained in a rigid transparent plastic tank of dimensions 30 cm × 30 cm × 5 cm, by exciting a paddle that is attached to a loudspeaker, as shown in the figure. The speaker is fed from an audio generator via a power amplifier. The quiescent height of water in the tank is maintained at approximately 4 cm., which is at least five times the wavelength at the lowest frequency used ($\simeq$30 Hz, see Fig. 2), to ensure operation in the deep-water regime. In order to optically monitor the surface waves, the tank is set up on a Fresnel lens that is part of a modified overhead projector. The modification consists of a Schlieren system in which a strobe lamp arrangement inside the box serves as the optical source. This source not only illuminates the waves, but also enables us to "freeze" the propagating surface waves in time by synchronizing the strobe lamp with the signal generator driving the speaker. The Fresnel zone plate in the Schlieren system focusses the strobe lamp onto a lens L, which images the surface, via mirror M, onto a vertical translucent screen. A stop S on the lens L ensures a dark Schlieren system by reducing the background illumination and thereby improving the contrast. Finally, a camera behind the screen records the "frozen" images of the propagating waves. Care is taken to ensure that the paddle/loudspeaker structure does not have resonances within the operating frequency range ($\simeq$30 to 100 Hz).

The technique described above gives a fair qualitative insight into the nature of the phenomena under investigation. For a quantitative measurement of the wave shapes, we measure the change in resistance between a ground plane and a dc probe touching the surface of the water. The detector probe thickness is chosen to be sufficiently smaller than the lowest wavelength of operation so that its "effective" diameter[5] remains small enough to ensure a reasonable spatial resolution. The dc bias to the probe is provided by a 9-V battery in series with a 10-K resistor and the probe is made to dip about 1.5 to 2 mm below the quiescent surface level of the water, as a compromise between sensitivity and linearity. Constant depth of immersion (and hence sensitivity) is ensured by monitoring the dc level at the probe tip under quies-

 0031-9171/82/111938-06$1.90

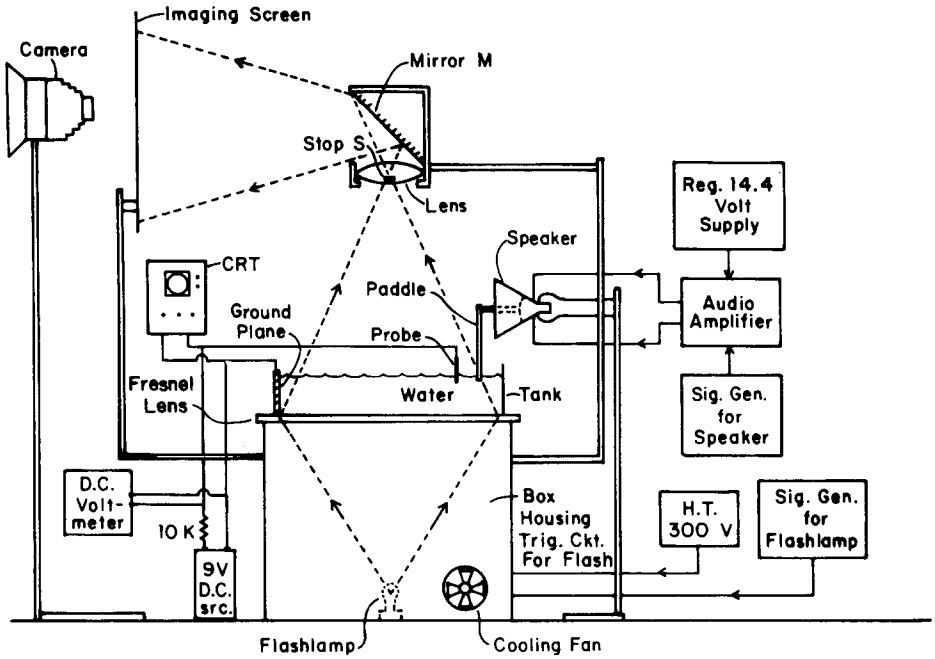

FIG. 1. Experimental setup used to study wave phenomena in water.

cent conditions.

In this connection it may be remarked that the resistance probe method was chosen in favor of a laser beam reflection technique[5] because the latter required a precise and difficult aligning procedure.

In order to test the system, the paddle was first excited at low amplitudes over a frequency range of 30 to 100 Hz and the ensuing plane-wave pattern observed. Dispersion characteristics were measured on photographs of the wave pattern [Fig. 3(a)]. The dispersion curve obtained (Λ vs f) was well in agreement with the theoretical predictions shown in Fig. 2.

Attenuation characteristics were also measured at different frequencies. The attenuation constant varied from 0.06/cm to 0.14/cm over a frequency range of 30 to 100 Hz in the case of reasonably clean tap water. However, in the presence of surface dirt, the attenuation constant was higher; indeed, within three days of filling the tank with "untreated" tap water, the attenuation constants were found to have increased to almost three times the corresponding values for clean water.

As the amplitude of the fundamental was slowly increased, subharmonic generation set in above a certain threshold fundamental amplitude. This could be detected on the screen by "freezing" the waves at half the fundamental frequency, i.e., at $\omega_p/2$, and is shown in Fig. 3(b). "Freezing" the waves at a quarter of the fundamental frequency reproduced the same result; furthermore, the distance between successive wavefronts of the suspected subharmonic approximately agreed with the value of Λ corresponding to $\omega_s = \omega_p/2$ in Fig. 2.

For a further verification of the threshold effect in subharmonic generation, the propagating waves were monitored using the probe discussed in the previous section. The wave patterns were observed on an oscilloscope at points in front of and to the side of the paddle. The observations are shown in Fig. 4. While the wave patterns in front of the paddle distinctly show the fundamental at all times [Fig. 4(a)], the patterns to the side of the paddle show virtually nothing [Fig. 4(b)] below a certain fundamental amplitude. Above this amplitude, or the threshold, the subharmonic is generated [Fig. 4(c)] and grows if the fundamental amplitude is increased.

III. THEORY

Following Phillips[1] and McGoldrick,[3,4] the conditions under which three waves can exchange energy among themselves in quadratic resonant interactions can be written as:

$$\omega_1 \pm \omega_2 \pm \omega_3 = 0, \tag{1}$$

$$\bar{k}_1 \pm \bar{k}_2 \pm \bar{k}_3 = 0, \tag{2}$$

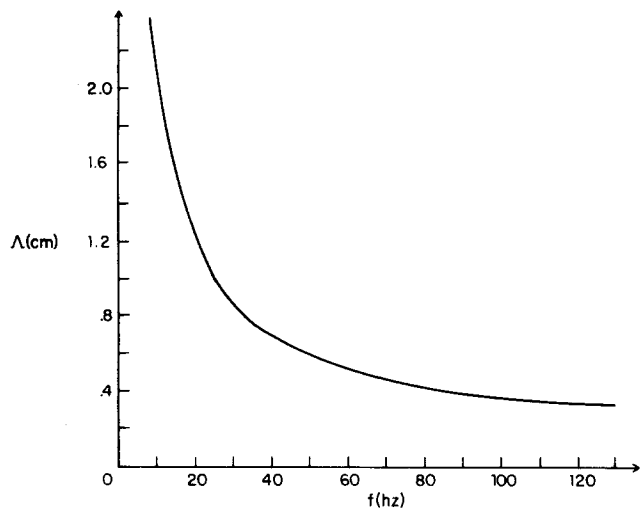

FIG. 2. Variation of the wavelength Λ with frequency f for capillary-gravity waves.

with

$$\omega_i = \omega_i(\bar{k}_i), \quad i = 1,2,3, \tag{3}$$

where ω represents the frequency and $\bar{k}$ the corresponding wavevector for the interacting wave. The wavevector triangle is shown in Fig. 5(a) for the general case and in Fig. 5(b) for the degenerate case where $\omega_1 = \omega_2$, $|k_1| = |k_2|$. From Fig. 5(b), (1,2, = s; 3 = p), it follows that the semiangle α between the propagating subharmonics $\bar{k}_1$ and $\bar{k}_2$ is given by

$$\alpha = \cos^{-1}(k_3/2k_1) = \cos^{-1}(\Lambda_1/2\Lambda_3), \tag{4}$$

where k_3 corresponds to ω_3, the fundamental frequency. Alternatively,

$$\alpha = \sin^{-1}(k_{1x}/k_1) = \sin^{-1}(\Lambda_1/\Lambda_{1x}), \tag{5}$$

(a)

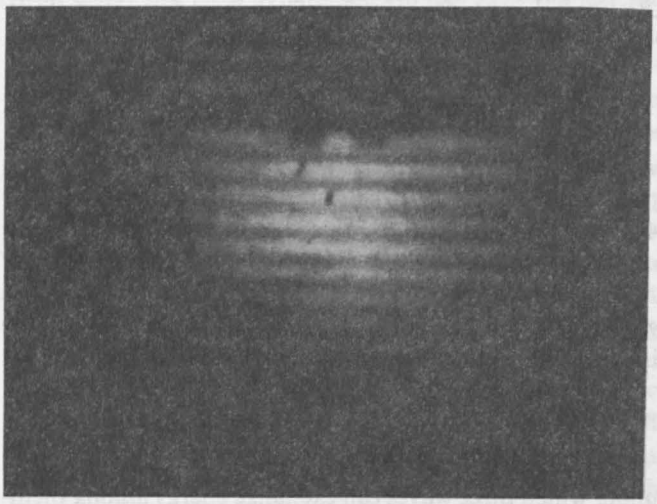

(b)

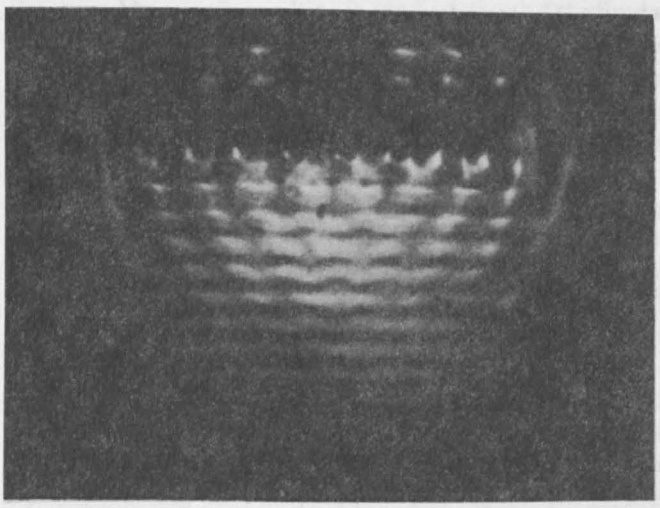

FIG. 3. (a) Plane wavefronts of the fundamental at low amplitudes on the water surface ($f_p = 60$ Hz); (b) Subharmonic generation as the fundamental amplitude is increased to above threshold. In both pictures, the paddle is at the top.

where k_{1x}, $k_{2x}(= -k_{1x})$ are the x components of the subharmonic propagation vectors parallel to the paddle.

If three waves, forming a resonant triad, are present the equation of the free surface can be expressed as:

$$\xi(x,t) = \sum_{i=1}^{3} a_i(t)\cos\psi_i,$$

where

$$\psi_i = \bar{k}_i \cdot \bar{x} - \omega_i t + \epsilon_i. \tag{6}$$

(a)

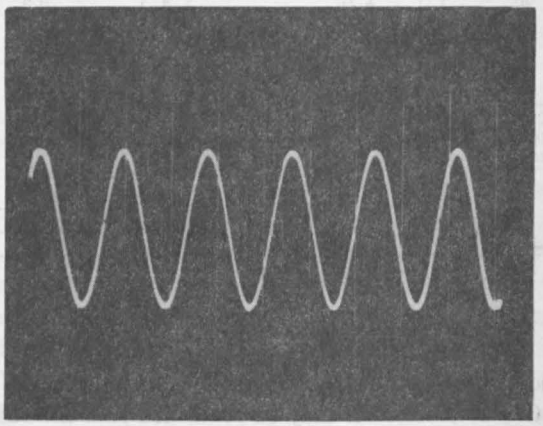

(b)

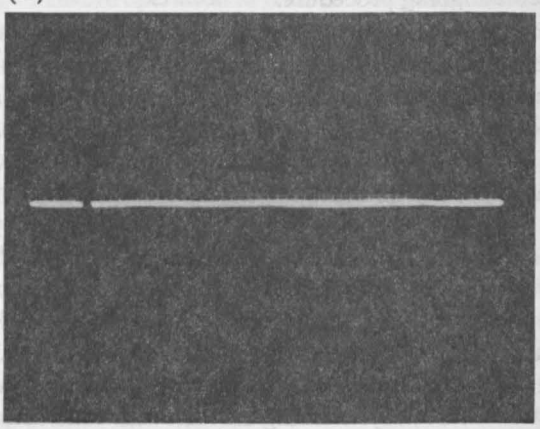

(c)

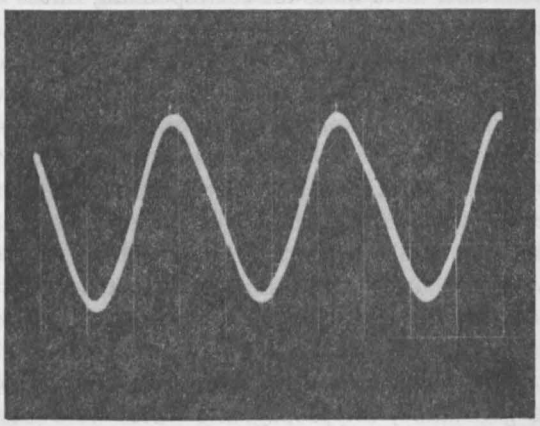

FIG. 4. Wave patterns detected by the resistance probe (a) in front of the paddle below threshold, (b) to the side of the paddle below threshold; (c) as (b) but above threshold.

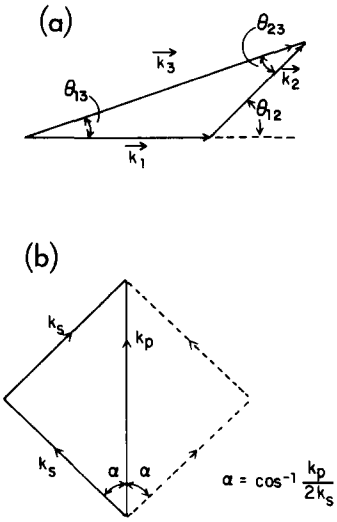

FIG. 5. Resonant wavevector triangle in the (a) general and (b) degenerate cases, respectively.

It can be shown[3] that the interacting amplitudes obey the following coupled set of equations:

$$\dot{a}_i \cos\psi_i = a_j\, a_k B_{jk} \sin(\psi_i + \gamma_i), \qquad i \neq j, \quad i,j,k: \ 1,2,3, \tag{7}$$

where the dot represents differentiation with respect to time and $B_{jk} = B_{jk}(k_1,k_2,k_3,\omega_1,\omega_2,\omega_3,T,\theta_{jk})$ where θ_{jk} is the angle between $\vec{k}_j$ and $\vec{k}_k$.

For the degenerate case, $\omega_1 = \omega_2 = \omega_3/2$; $|\vec{k}_1| = |\vec{k}_2|$; $\gamma_1 = \gamma_2$; $a_1 = a_2$; $B_{13} = B_{23}$. Also, to ensure growth of the subharmonic (viz., a_1) we choose $\gamma_1 = \pi/2 = -\gamma_3$ so that the coupled equations (4) become:

$$\dot{a}_1(t) = B_{13} a_1 a_3, \tag{8}$$

$$\dot{a}_3(t) = -B_{12} a_1^2. \tag{9}$$

Substituting

$$a_1 = (B_{12}B_{13})^{-1/2}\bar{a}_1, \tag{10}$$

$$a_3 = B_{13}^{-1}\bar{a}_3 \tag{11}$$

into (8) and (9), we obtain the following normalized set of coupled equations:

$$\dot{\bar{a}}_1 = \bar{a}_1\bar{a}_3, \tag{12}$$

$$\dot{\bar{a}}_3 = -\bar{a}_1^2. \tag{13}$$

Assuming that the subharmonic generation starts at the noise level, our initial conditions become:

$$\bar{a}_3(t=0) = \bar{A}_{30}, \tag{14}$$

$$\bar{a}_1(t=0) = \bar{A}_{10} = \epsilon\bar{A}_{30}, \tag{15}$$

where $\epsilon\bar{A}_{30}$ represents the initial noise condition.

Using (12)–(15), it may be readily shown that

$$\bar{a}_1^2(t) + \bar{a}_3^2(t) = \text{const} = \bar{a}^2 = (1+\epsilon^2)\bar{A}_{30}^2. \tag{16}$$

Using (12), (13), and (16), and integrating, we obtain, after some algebra,

$$\bar{a}_1(t) = \bar{a}\ \text{sech}\ \bar{a}(t - t_0), \tag{17}$$

$$\bar{a}_3(t) = -\bar{a}\ \tanh\bar{a}(t - t_0), \tag{18}$$

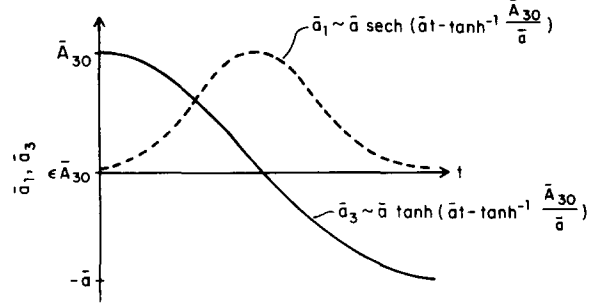

FIG. 6. Theoretically predicted variations of the subharmonic ($\bar{a}_1$) and fundamental ($\bar{a}_3$) amplitudes with propagation time.

where

$$t_0 = \bar{a}^{-1}\tanh^{-1}(\bar{A}_{30}/\bar{a}) \simeq \bar{A}_{30}^{-1}\ln(\epsilon^{-1}). \tag{19}$$

The time variation of $\bar{a}_1(t)$ and $\bar{a}_3(t)$ is shown in Fig. 6. Note from Eqs. (17) through (19) that at $t = 0$, $\bar{a}_1 = \epsilon\bar{A}_{30}$ and $\bar{a}_3 = \bar{A}_{30}$; at $t = t_0$, $\bar{a}_1 = \bar{a}_{1\max} = \bar{a}, \bar{a}_3 = 0$ and as $t \to \infty$, $\bar{a}_1 \to 0$, $\bar{a}_3 \to -\bar{a}$.

For small t, we may write, using (17) and (19),

$$\bar{a}_1 \simeq \epsilon\bar{A}_{30}\exp(\bar{A}_{30}t). \tag{20}$$

Now the viscous dissipative forces in the medium may be represented by $\exp(-2\nu k_1^2 t)$ for the subharmonic where ν is the coefficient of dynamic viscosity. Hence, for the subharmonic to grow at all, we must impose

$$\bar{A}_{30} > 2\nu k_1^2,$$

or

$$A_{30} > 2\nu k_1^2/B_{13}, \tag{21}$$

which defines the threshold.

IV. EXPERIMENTAL RESULTS

From the picture in Fig. 3(b) it appears that above threshold, the subharmonic forms a standing wave pattern along the paddle. To verify this, the interacting waveshapes were monitored by moving the probe parallel to the paddle at

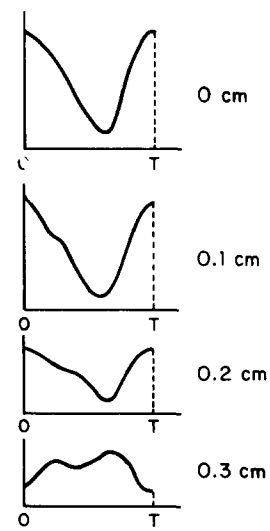

FIG. 7. Typical waveforms (over half a cycle) measured by the resistance probe moving parallel to the paddle.

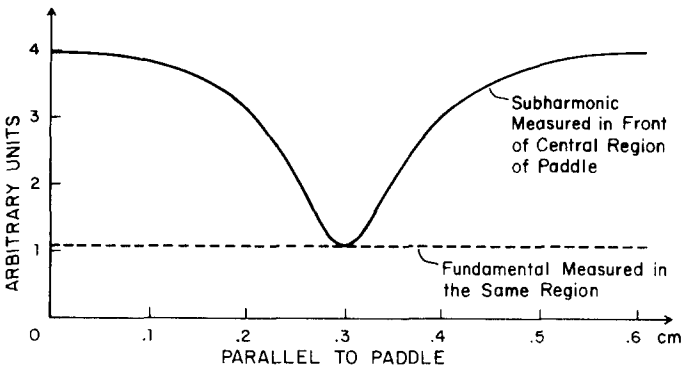

FIG. 8. Measured variation of fundamental and subharmonic amplitudes with distance parallel to the paddle.

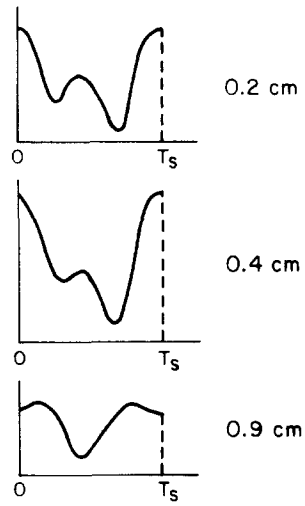

FIG. 10. Typical waveforms measured by the resistance probe moving perpendicular to the paddle.

a distance of approximately 0.3 cm in front of it. Typical waveshapes are shown in Fig. 7. The amplitudes of the interacting frequencies were deduced by determining the Fourier coefficients of the waveform at each observed point on the water. This was done numerically on a computer by sampling the periodic waveform at eight times its fundamental or repetition frequency and using a 8-point Fast Fourier Transform (FFT) algorithm.[6] The variation of the fundamental and subharmonic amplitudes for a fundamental frequency of 60 Hz is shown in Fig. 8. The actual ratios between these amplitudes may differ by a constant factor from the experimental values due to reduced frequency sensitivity of the probe at higher frequencies.[5] Note that the subharmonic indeed forms a standing wave pattern while the fundamental amplitude is fairly constant. This is in agreement with the theory of interactions discussed in the previous section as only the propagating subharmonics have contradirected wavevector components viz., $k_{1x}, k_{2x} (= -k_{1x})$, parallel to the paddle that may form a standing wave pattern of period $\Lambda_{1x}/2$. The distance between consecutive peaks, $\Lambda_{1x}/2$ in Fig. 8, corresponds to the distance between consecutive bright regions along the paddle in the picture of Fig. 3(b).

Having confirmed the existence of standing waves, the semiangle α between the propagating subharmonic wavetrains was calculated by measuring the standing wave period at various fundamental frequencies and employing Eq. (5). The variation of α with frequency is shown in Fig. 9 along with the theoretical curve, as predicted by Eq. (4) and the dispersion curve (Fig. 2). The systematic difference between experimental and theoretical values may be due to the fact that the dispersion curve is amplitude dependent through the cubic nonlinearity, not considered here.

To determine the value of the threshold, recall that around 30 Hz, the measured value of the attenuation constant is about 0.06/cm for clear water, or 1.44/sec. This is in good agreement with the theoretical value $2\nu k_1^2 = 1.2/\text{sec}$ ($\nu = 0.01$ cm^2/sec) at the same frequency. Using (21) and assuming[3] $B_{13}/\omega_1 k_1 \simeq 0.1$, the fundamental amplitude at threshold, A_{30}, is of the order of 0.10 mm for clean water, while for dirty water, it should be about three times higher. From our experimental data, at the onset of threshold the paddle moves by approximately $\pm$ 1.0 mm from its equilibrium position; and its depth of immersion in water is about 3

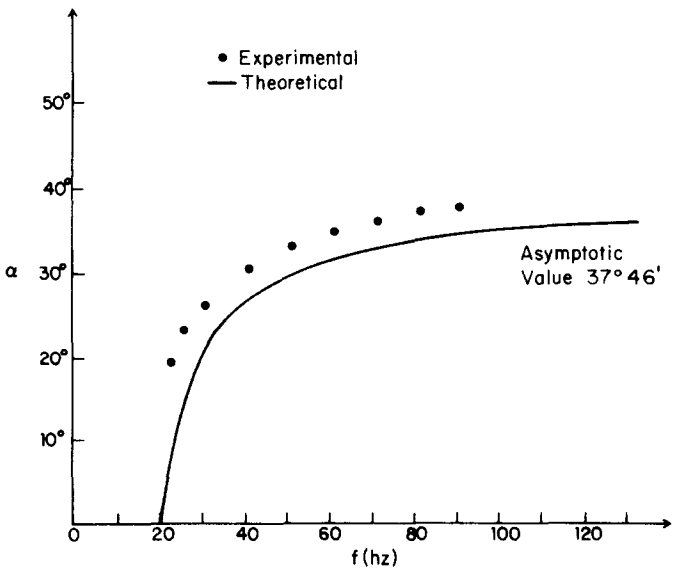

FIG. 9. Theoretical and experimental values of the interaction angle α as a function of frequency.

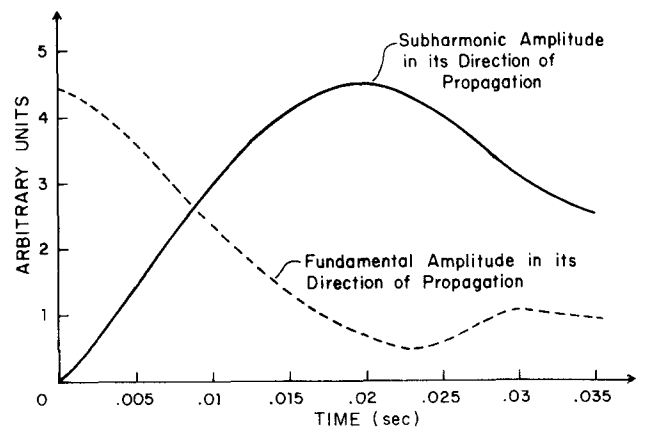

FIG. 11. Measured variation of fundamental and subharmonic amplitudes with propagation time.

mm. This appears not to be too incompatible with calculated threshold values. We have however found that, if anything, the threshold is lower rather than higher in dirty water. The cause of this is not known at present.

Finally, the variation of the fundamental and subharmonic amplitudes with propagation time was determined in the following way. The waveshapes were monitored by the probe at various distances perpendicular to the paddle. Typical waveshapes are shown in Fig. 10. Using the FFT algorithm mentioned above, the fundamental and the subharmonic amplitudes were calculated. Their variation with propagation time was derived from a knowledge of their propagation velocity and the semiangle α at a particular frequency. The results for a fundamental frequency of 60 Hz is shown in Fig. 11. A comparison with Fig. 6 brings out the qualitative similarities, i.e., the subharmonic attaining a maximum when the fundamental goes through a minimum. Regeneration of the fundamental occurs after this, although the losses in the medium finally force it to decay.

V. CONCLUSIONS

In conclusion, we have observed and analyzed subharmonic generation of deep-water capillary waves due to resonant noncollinear three-waves interactions and found substantive agreement between theory and experiment.

ACKNOWLEDGMENT

The authors acknowledge the support of the National Science Foundation under Grant No. ENG-7902889.

[1]O. M. Phillips, J. Fluid Mech. **9**, 193 (1960).
[2]M. S. Longuet-Higgins and N. D. Smith, J. Fluid Mech. **12**, 321 (1962).
[3]L. F. McGoldrick, J. Fluid Mech. **21**, 305 (1965).
[4]L. F. McGoldrick, J. Fluid Mech. **40**, 251 (1970).
[5]G. V. Sturm and F. Y. Sorrell, Appl. Opt. **12**, 1928 (1973).
[6]A. V. Oppenheim and R. W. Schafer *Digital Signal Processing* (Prentice-Hall, NJ, 1975), p. 330.